Pharm Res (2014) 31:2549–2558
DOI 10.1007/s11095-014-1352-0

RESEARCH PAPER

Dipole-Dipole Interaction in Antibody Solutions: Correlation with Viscosity Behavior at High Concentration

Shubhadra N. Singh • Sandeep Yadav • Steven J. Shire • Devendra S. Kalonia

Received: 9 October 2013 / Accepted: 27 February 2014 / Published online: 18 March 2014

ABSTRACT

Purpose The purpose of this study was to investigate the contribution of the dipole moment to overall protein-protein interactions and viscosity of a monoclonal antibody MAb1.

Methods The dipole moment of MAb1 was measured at various solution pH conditions using dielectric relaxation spectroscopy.

Results The dipole moment for MAb1 was highest at pH 6.5, and the pH dependent change in molecular dipole correlated fairly well with previously observed trends of viscosity and storage modulus *versus* pH. Moreover, the magnitude of the dielectric increment at pH 6.5 and 7.0 showed strong concentration dependence, indicating the presence of relatively strong dipole-dipole interactions at these pHs. To test if the cluster of charged residues present in the Fab contributes to the mean dipole moment observed for MAb1, additional mutants involving charge mutations in the CDR were investigated. In contrast to MAb1, all of the other MAbs showed significantly reduced pH and concentration dependence of the measured dipole moments and dielectric increments, respectively.

Conclusions The solution pH dependent measured dipole moments of MAb1 appears to be in line with the observed intermolecular interactions and viscosity behavior suggesting that dipole-dipole interaction plays an important role in governing the high concentration solution behavior of this MAb.

S. N. Singh
Process and Formulation Development, Olympus Biotech Corporation
Lebanon, New Hampshire, USA

S. N. Singh • D. S. Kalonia (✉)
Department of Pharmaceutical Sciences, University of Connecticut
69 N Eagleville Road, Storrs, Connecticut 06269, USA
e-mail: kalonia@uconn.edu

S. Yadav • S. J. Shire
Late Stage Pharmaceutical Development, Genentech Inc.
South San Francisco, California, USA

KEY WORDS dielectric relaxation spectroscopy · dipole interactions · high concentration solutions · self-association · short-range interactions

INTRODUCTION

The use of high concentration formulations of monoclonal antibodies (MAbs) and MAb-like proteins has grown rapidly in recent years (1,2). Many diseases that are being targeted by MAbs requiring mg/kg dosing, are chronic and require frequent dosing, providing an at home-outpatient administration option to patients by the subcutaneous (SC) route, which is desirable to increase patient compliance. The volume limitation (<1.5 mL) presented by the SC delivery route necessitates that the antibody and IgG-like therapeutics be formulated at high concentrations (>100 mg/mL). However, there are several challenges associated with the development of such high concentration solutions. At high concentrations, the tendency of protein molecules to self-associate and/or form higher order aggregates increases due to increased interactions between protein molecules caused by decreased intermolecular distances. These increased intermolecular interactions may also result in solubility and viscosity issues. Aggregation, solubility and viscosity issues associated with the development of concentrated protein solutions substantially increase the complexity of preparing and administering such formulations (2–4). Enhanced aggregation propensity may further lead to additional problems of loss of potency, altered pharmacokinetics, decreased shelf life and enhanced immunogenicity (5–8).

Static and dynamic light scattering techniques have been frequently used to characterize protein-protein interactions in dilute protein solutions. The results and trends have often been observed to have good correlation with the aggregation behavior of antibodies at high concentrations (9–11). Static light scattering determines the second virial coefficient (B_{22}), a

measure of the solution's deviation from non-ideality and comprises the effect of excluded volume and net interactions of all solute particles (12,13). Dynamic light scattering on the other hand provides the interaction parameter (k_D), which incorporates the effects of B_{22}, the partial specific volume, and a frictional coefficient (14–16). The two techniques have been used to predict the solution conditions favorable for protein solubilization and precipitation (crystallization and/or amorphous) (12). Recent literature however suggests that forces in addition to charge-charge interactions that become significant under concentrated conditions may result in a change in the kinetics of reactions such as aggregation. For example, minimization of the colloidal repulsive interactions at very high concentrations may lead to a change in the rate limiting step (conformational stability becoming rate limiting). Clearly, it very difficult to predict rheological and/or stability behavior of the concentrated solutions based on extrapolated data generated at low concentrations (17–20).

The concentration dependency of the viscosity of MAb1, which is the antibody used in the studies reported here, has been previously characterized by Liu *et al.* (4). In this study, the concentration dependent reversible self-association of MAb1 was observed at pH 6.0. Additional studies by Kanai *et al.* (3) indicated that the self-association originates from intermolecular Fab-Fab interactions. Decrease in self-association behavior of MAb1 in the presence of salts or ions led these authors to believe that the self-association was electrostatic in nature. Studies by Yadav *et al.* (11,21), suggested that a cluster of charged residues located on the Fab domain of MAb1 may promote charge-dipole and dipole-dipole attractive interactions leading to self-association of MAb1. The fact that distribution of charge residues in the CDR contributes to viscosity and the self-associating behavior of MAb1 was subsequently strengthened by the observed non-associative nature of its charge-swapped mutant that lacked charged residues present on the surface of Fabs of MAb1 (22,23).

The purpose of this study was to measure the dipole moment of MAb1 under various solution conditions, and hence identify if short-range dipole interactions indeed contribute to the high viscosity and high attractive intermolecular interactions around pH 6.0 as observed earlier in several studies. The technique of dielectric relaxation spectroscopy was used to measure the dipole moments. The dielectric dispersion technique was originally developed by Oncley to study protein size and shape (24–26). Later, the technique was utilized to study the self-association of proteins in aqueous solutions (27,28). In this technique, the dielectric constant of a protein solution is measured as a function of frequency (10^5–10^8 Hz) in an alternating electric field. The protein dipoles are aligned with the electric field in the low frequency region and thus can be used to calculate the static dielectric constant, ε_0 (Fig. 1). This dielectric constant decreases with an increase in the frequency because the protein dipoles cannot keep pace with the constantly changing field. A stage is finally reached wherein protein molecules behave as nonpolar entities and do not contribute to the dielectric constant (this constant is hence known as the high frequency dielectric constant (ε_∞)). The polarizability of a protein or the difference between the static dielectric constant and the high frequency dielectric constant (dielectric increment) is proportional to the dipole moment of the protein molecule.

The role of dipole-dipole interaction, in the self-association behavior of MAb1 observed previously, was studied by measuring the dielectric increment as a function of concentration. In addition, the rotational relaxation time,τ, the time required for field oriented dipoles to become randomly distributed with increasing frequency, is an important parameter that was also obtained from such experiments. Furthermore, to understand the electrostatic interactions causing the self- association of this MAb it is necessary to understand the location and conformation of the charged residues that can dictate the geometry for these dipole-dipole interactions. To verify the role of the charged residues, another monoclonal antibody, MAb2 (the same MAb2 discussed in Liu *et al.* (4)) as well as two "charge-swap" mutants, M7 and M10, described in Yadav *et al.* (23) were studied. These MAbs (MAb1, MAb2, M7 and M10) differ in the number and location of charged residues in the complementarity (CDR) region as summarized in Table 1 of Reference 23. In order to probe the role of the individual surface charges that may contribute to dipole-dipole interactions, we determined the dipole moments of these MAbs by dielectric spectroscopy and investigated the distribution of electrostatic surface potential on the three dimensional models of these MAbs.

MATERIALS AND METHODS

Monoclonal antibodies (MAb1, MAb2 and their "charge-swap" mutants, M-7 and M-10) were supplied by Genentech Inc. (South San Francisco, CA) in 30 mM histidine buffer at pH 6.0. All other reagents were obtained from Fisher Scientific (Fair Lawn, NJ, USA). Buffers used to maintain the pH of antibody solutions were prepared using Milli-Q™ grade water. The pH was adjusted with 1.0 N HCl or NaOH and the buffers were then filtered through 0.1 μm filters (Millipore, Billerica, MA, USA). All buffers were prepared at a concentration of 2 mM to minimize the effect of electrode polarization. Stock solutions of antibodies were dialyzed against the desired buffer by using four dialysis cycles using 15 mL Millipore Amicon Ultra centrifugation concentration tubes with a molecular cutoff of 10 kDa. Buffering reagents used included acetic acid, sodium acetate buffer at pH 4.0,

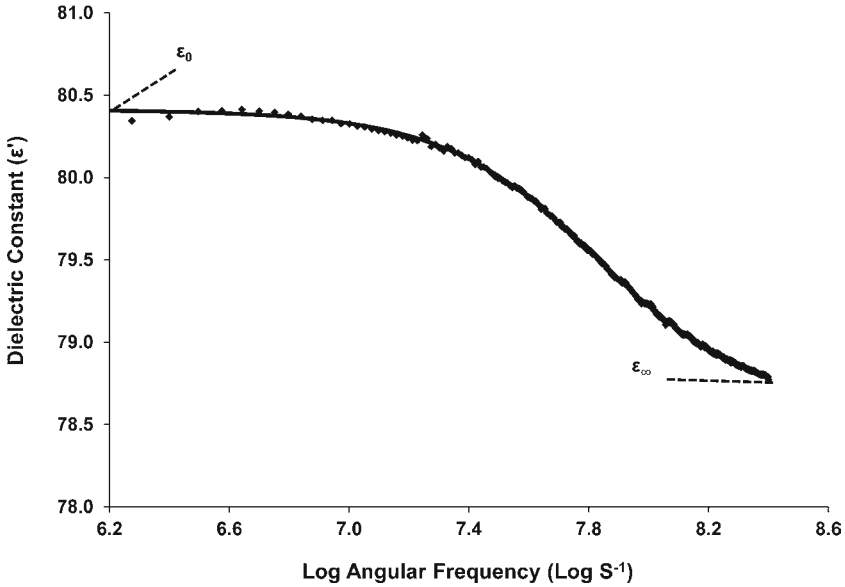

Fig. 1 Plot of dielectric constant *versus* the logarithm of angular frequency. The *triangles* represent the experimental values. The *solid line* was calculated by fitting the Cole-Cole equation to the experimental data. The ε_0 and ε_∞ are low frequency and high frequency dielectric constants.

Histidine –hydrochloride buffer at pH 6.0, phosphate for pH 7.0 and TRIS at pH 8.0 and 9.0. Concentrations of proteins solutions were determined by UV absorption using a Cary 50-Bio UV–Vis spectrophotometer (Varian Inc., Palo Alto, CA, USA). The concentrations of the MAbs were determined at 280 nm using extinction coefficients of 1.6 $(mg/mL)^{-1}cm^{-1}$ for MAb1 and M7, and 1.5 $(mg/mL)^{-1}cm^{-1}$ for MAb2 and M10.

Experimental Dipole Moment

The frequency domain technique was used to measure the dielectric constant. The experiments were performed at oscillation strength of 0.1 V, with four averaging times and medium integration from 100 Hz to 40 MHz to obtain the susceptance (B) and conductance (G) of the protein solutions. The value of the capacitance (C) was calculated by using the relationship between susceptance and capacitance ($B=\omega C$) as discussed by Chari et. al. (29). The major problem in determining the susceptance or capacitance of sample solutions is electrode polarization, which has a major impact at low frequencies due to the formation of an electric double layer on the electrode surface (Fig. 2). To correct for the effect of electrode polarization, the susceptance (or calculated capacitance) of a NaCl solution was measured and adjusted to nearly the same conductance as the sample solutions and the dielectric constant (ε_s) was calculated at each frequency using Eq. 1 (29):

$$\frac{\varepsilon_s-\varepsilon_a}{\varepsilon_w-\varepsilon_a}=\frac{B_s-B_a}{B_w-B_a} \tag{1}$$

where B_s, B_a, and B_w are the susceptance of protein, air and salt solutions, respectively, and ε_w and ε_a are the dielectric constants of water and air with values of 78.54 and 1, respectively. The calculated values of ε_s were plotted *versus* the logarithm of angular frequency (dispersion plot) as shown in Fig. 1. The real part of the Cole-Cole equation (Eq. 2) was iteratively fitted to the dispersion plot (30,31):

$$\varepsilon=\varepsilon_\infty+\frac{(\varepsilon_0-\varepsilon_\infty)\left\{1+(\omega\tau)^n\cos\left(n\pi/2\right)\right\}}{1+2(\omega\tau)^n\cos\left(n\pi/2\right)+(\omega\tau)^{2n}} \tag{2}$$

where τ is the relaxation time, ω is the angular frequency, $n=1-\alpha$ where α is the Cole-Cole distribution parameter, ε_∞ is the dielectric constant extrapolated at infinite frequency, and ε_0 is the dielectric constant extrapolated at zero frequency. The parameters ε_∞, ε_0, τ, ω, and α were varied until the equation plot converged with the experimental plot, thus enabling the determination of the dielectric increment, $\Delta\varepsilon=\varepsilon_0-\varepsilon_\infty$

The dipole moment, μ, was then calculated using the modified Oncley's equation (29,32,33):

$$\mu=\sqrt{\frac{9kTM_w\varepsilon_p(\varepsilon_0-\varepsilon_\infty)}{1000N_Ahc}} \tag{3}$$

where k is the Boltzmann constant (J/K), T is the temperature (K), Mw is the protein molecular weight (g/mole), ε_p is the permittivity constant for vacuum ($C^2J^{-1}\ m^{-1}$), N_A is Avogadro's number, ε_o and ε_∞ are the dielectric constants extrapolated at zero and infinite frequency, respectively (unitless since these are relative to the dielectric constant of vacuum), c is the protein mass concentration (mg/ml) of protein and h is a dimensionless constant that ranges from 4.0 to 5.8 and contains the Kirkwood correlation factor, g (34). μ has units of C·m and is converted to Debye units (D) by multiplying by 2.998×10^{29}.

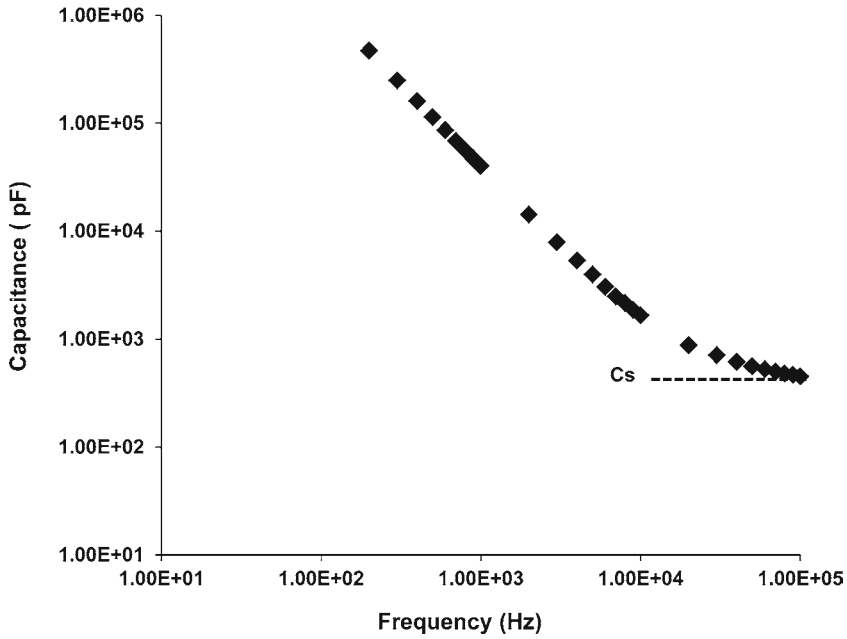

Fig. 2 The log-log plot of capacitance *versus* frequency. The *curve* shows a sharp increase in the capacitance below 100 KHz due to the electrode polarization effect. The *horizontal broken line* represents true sample capacitance (Cs).

Electrostatic Surface Potential

To determine the electrostatic properties of the MAbs, the adaptive Poisson Boltzmann Solver (APBS) program (35) was used. The MAb1 model was generated using the x- ray coordinates of Fab and Fc crystal structures that were obtained from the protein data bank (Brookhaven, NY, identity codes 1N8Z and 3DG6, respectively). X-ray coordinates of the Fab domain of MAb2 were provided by Genentech Inc. (data not published). Coordinates of 3DG6 were used for the MAb2 Fc since its Fc domain is identical to the Fc domain of MAb1. Prior to computational analysis, the PDB structures were prepped with the molecular modeling programs Discovery Studio 2.1 (Accelrys, Inc., San Diego, CA, USA) or Hyperchem Professional 7.5.1 (Hypercube, Inc., Gainesville, FL, USA). The coordinates of the heavy chain portion between the Fab and Fc, commonly known as the hinge region are not available in the PDB data bank. To construct the hinge region, two parallel 19 amino acid segments were constructed in an extended conformation with a central core sequence Cys-Pro-Pro-Cys using Hyperchem Professional 7.5.1. The central cysteine residues were connected to form disulfide bonds and energy minimization was done on the central part, holding all of the other residues fixed. The amino terminal residues of the hinge region were connected to the Fab arms (2 Fabs) and C-terminal residues were connected to the two Fc domains (*via* formation of peptide bonds) to complete the models of the antibodies. Finally, the connecting residues and residues within 6 Å of connecting residues were moved until the structures converged to a minimum energy state. All protein and antibody structures were saved in PDB format. The M7 and M10 structures were generated by changes in the appropriate amino acids followed by minimization of energy. Since the APBS program requires a PQR file, which provides the charge and radius information for every atom and an input file, these files had to be generated. The PQR file was generated by using an in-house program that uses the PDB file as input (29), and the input file was obtained with the program PDB2PQR (36), and is centered on a $160 \times 160 \times 160$ grid with dimension of each side of the sub-unit equaling 1.4 Å. An interior dielectric of 4, exterior dielectric of 80 and 0.010 M salt concentration was used in the calculation. Finally, the software VMD was used to color code the molecular surface of the MAbs, and create a 3D graphical representation of each protein (37).

RESULTS AND DISCUSSION

Correlation of Experimental Dipole Moment with G' and k_D

The experimental dipole moment of MAb1 was obtained over a pH range of 4.0–9.0 (Fig. 3). The magnitude of the dipole moment of MAb1 increased from pH 4 to 6.5 and decreased sharply from pH 7.0–9.0 showing the highest dipole moment at pH 6.5. In contrast the experimentally determined dipole moment for a monoclonal antibody, MAb2, with the same IgG1 human Fc framework as MAb1 but differing in 20 residues located in the CDRs peaks somewhere between pH 7 and 8 (Fig. 3), and is considerably lower in value at pH 6.5. Previously it had been shown that MAb1 at 125 mg/mL at 25°C had a maximum value for the determined storage modulus, G', at ~pH 6 at low ionic strength determined with

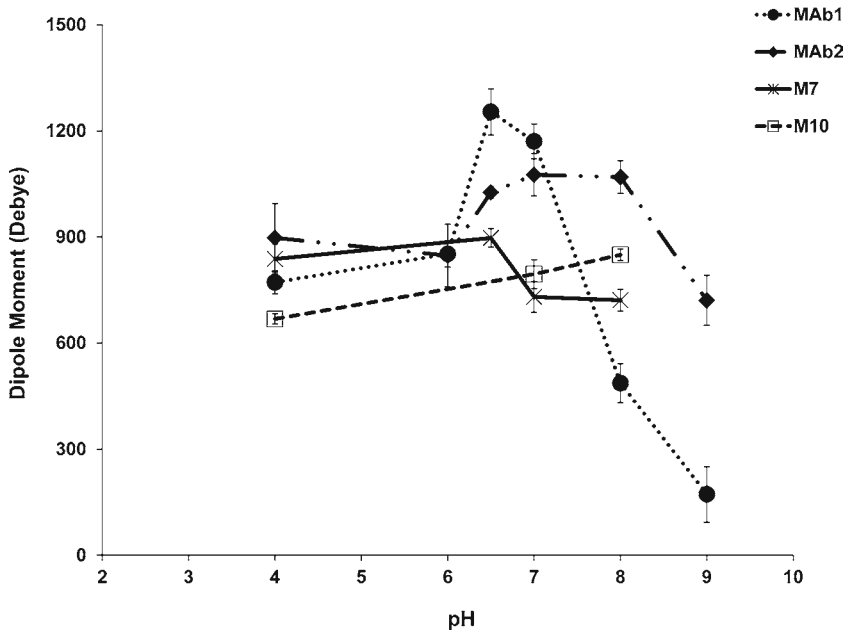

Fig. 3 Experimental dipole moments *versus* pH of MAb1, MAb2, M7 and M10.

a high frequency quartz rheometer (11). The storage modulus reflects the strength of attractive protein-protein interactions (19), which is corroborated by the negative values of the interaction parameter, k_D, for MAb1 at pH 6 and low ionic strength as determined by dynamic light scattering measurements (11). The determined dipole moments for MAb2 as a function of pH are also consistent with previously determined G' and k_D values which are maximum at ~pH 8. These observed pH trends of G' and k_D also correlate with the pH dependency of viscosity for MAb1 and MAb2 (4,11), suggesting that dipole interactions contribute to the rheological properties of these MAbs at high concentration.

Role of Charged Residues on the Magnitude of Dipole Moment and Viscosity

To explore the role of charged residues on dipole moment and viscosity, charge-swap mutants for MAb1 and MAb2 were produced. In these mutants eight residues located in the light and heavy chains of the CDRs of MAb1 were replaced by neutral residues accommodated in the structure of MAb2 to generate M7, and similarly eight uncharged residues present in the CDRs of MAb2 were replaced by the charged residues at their respective positions as found in the CDR of MAb1 to generate M10 (23). Previously it was shown that at pH 6 and low ionic strength the viscosity increase with concentration followed the trend of (MAb1 > MAb2 ≃ M7 ≃ M10) (23). Overall, the purpose of studying the charge-swap mutants was to determine if the pH dependent protein-protein interactions and viscosity behavior observed for these MAbs can be accounted for by the presence and pH dependency of large magnitude dipole moments, and whether specific localization of charged surface residues in the CDRs results in such dipole-dipole or charge-dipole interactions. The measured values of the dipole moments for the MAbs and the charge- swap mutants, MAb1, MAb2, M7 and M10 (described in Table I in Yadav *et al.* (23)) as a function of pH are shown in Fig. 3. Though the dipole moment *versus* pH trend for M7 was similar to MAb1, the magnitudes of the dipole moments for M7 at pH 6.5 and pH 7 were drastically reduced suggesting importance of charged residues in the CDR region of MAb1. For MAb2, the dipole moment decreased from pH 4 to 6, increased from pH 6 to 8 followed by decrease at pH 9. In the case of M10, the dipole moment increased from pH 4 to 8. Since M10 was generated by replacing the uncharged residues in MAb2, it can be seen that only a few amino acid differences among MAbs produce drastic differences in the dipole moment values and in the pH *versus* dipole moment trend.

Mechanism of Dielectric Dispersion

Several theories including the rotation of permanent dipoles (26,38,39), proton fluctuations, Maxwell-Wagner (40) and ion mobility mechanisms (41) have been proposed to explain the dipole moment of a protein. According to the theory of permanent dipoles, a dipole moment can be wholly accounted for by charge anisotropy. Charge anisotropy refers to the presence of a cluster of positively charged residues (Lys, Arg) on one end and negatively charged residues (Asp,Glu) on the other end of the protein. Out of all the MAbs, MAb1 shows the highest charge asymmetry because of the presence of a large number of negatively charged residues on the CDRs of the Fab domain and positively charged residues on the CH3 region of the Fc domain (Fig. 5 at pH 7 and Fig. 4 at pH 6 in Yadav *et al.* (22)). For MAb1, a significant increase in the magnitude of the dipole moment is expected between pH 4

and 8 because of the increase in the negative charge (on the CDRs) following dissociation of aspartic and glutamic acid residues (pKas ≈ 3–5). However, the absence of a comparable dipole moment *vs*. pH profile for M10 that has similar charged residues in the CDRs suggests a less asymmetric distribution of charges in M10 compared to MAb1 as shown here in Fig. 4 and Fig. 4 in Yadav *et al.* (22). The dipole orientations of the MAbs seem to correspond to the development and change in the electrostatic surface potential. The red contour in space represents the location of the −1 kT/e potential surface while the blue contour shows the location of the +1 kT/e potential surface. At pH 7, as shown by the red contour in Fig. 4a, the wild type MAb1 displays a large anionic lobe of negative potential induced by ionization of Asp and Glu residues. In the case of the other MAbs, this large lobe of anionic potential decreases (Fig. 4b–d). Even the MAbs that were generated from the same human IgG1 framework exhibited different electrostatic surface potential. The differences in the electrostatic surface potential may result in differences in asymmetric distribution of charges among antibodies and hence the magnitude of the dipole moments.

Dielectric Increment *Versus* Dipole Moment for MAb1, MAb2, M7 and M10

The dielectric increment obtained as a function of concentration, and extrapolated to zero concentration was used to determine the dipole moments of the MAbs through Oncley's equation (Eq. 3). The concentration dependence of the dielectric increment as a function of concentration is shown in Fig. 5a–d. For Mab1, the dielectric increment at pH 6.5 and 7.0 decreased with an increase in the concentration (Fig. 5a and b). On the other hand, M7 did not show any significant concentration dependence. MAb2 showed some decrease in dielectric increment with an increase in concentration, but due to scatter in the data, no justifiable conclusion can be drawn. Similar to M7, M10 also does not show any concentration dependence. The concentration dependence of the dielectric increment for MAb1 can be explained by the ordering of the protein dipoles. The effect of orientation or ordering on the Kirkwood correlation factor in Oncley's Eq. 3 is given by (34):

$$g = 1 + \mathcal{Z}^{*}(\cos\gamma) \tag{4}$$

where Z* is the number of nearest neighbors surrounding the dipole, and cos γ is the mean value of the cosine of the angle between dipole moments. In Oncley's equation g, the Kirkwood correlation parameter, is assumed to be 1 and therefore, the dielectric increment has been considered to be independent of the intermolecular dipole interactions. Though this assumption may hold true in dilute solutions, where dipoles move freely, our results and those obtained by Debye *et al.* (42) demonstrate that intermolecular interactions can cause deviation from this ideal behavior. Clearly, the value of g will be more than one in the case of parallel alignment of dipoles and less than 1 in the case of anti-parallel alignment of dipoles. The slope resulting from the plot of the dielectric increment *versus* concentration will hence be positive when there is parallel alignment and negative when there is antiparallel arrangement of dipoles. Oleinikova *et al.* (43) have shown that an antiparallel arrangement of protein molecules is favored

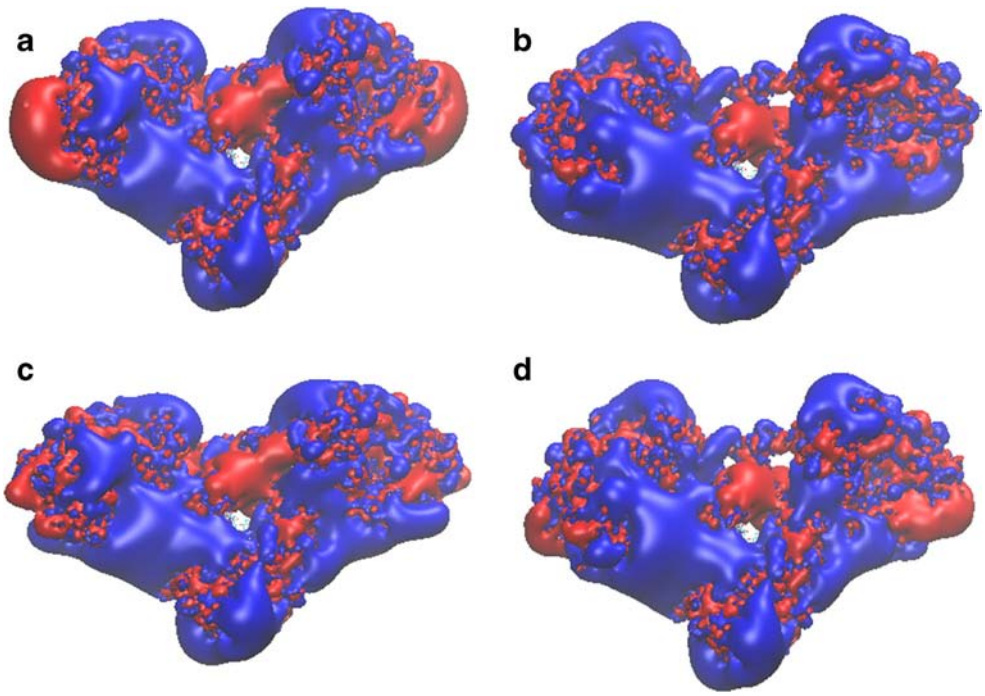

Fig. 4 Electrostatic potential surfaces of (**a**) MAb1, (**b**) M7, (**c**) MAb2 and (**d**) M10 at pH 7 and 10 mM ionic strength. *Blue contours* represent the spatial distribution of +1 kT/e potential. *Red contours* represent the spatial distribution of −1 kT/e potential.

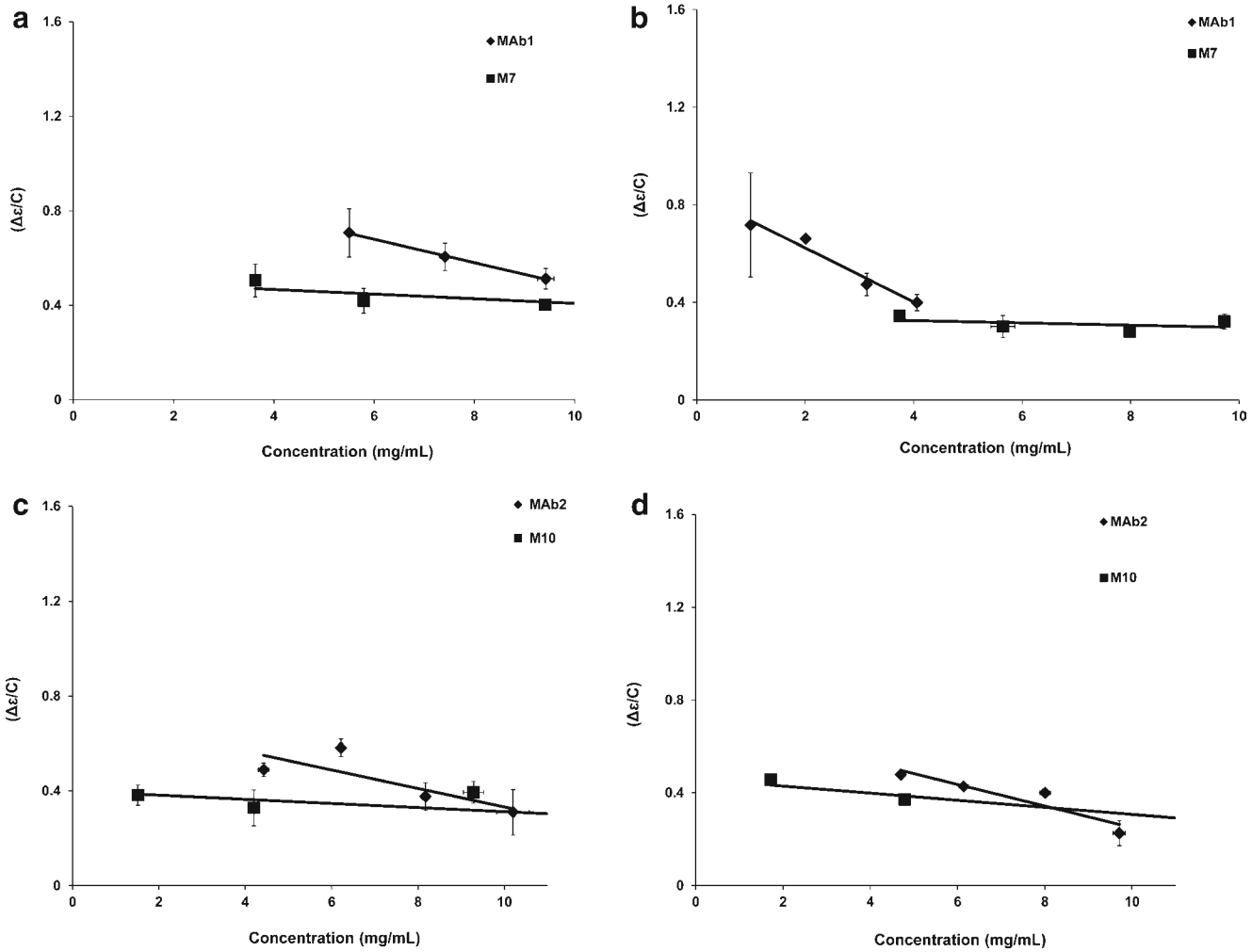

Fig. 5 The effect of concentration on dielectric increment of MAbs. (**a**) MAb1 and M7 at pH 6.5 (**b**) MAb1 and M7 at pH 7.0 (**c**) MAb2 and M10 at pH 7 and (**d**) MAb2 and M10 at pH 8.0.

when the magnitude of the dipole moment is high (negative value of g). The decrease in the dielectric increment (negative slope), for MAb1 between pH 6 and 7, with an increase in concentration can hence be explained as follows. Under dilute conditions, the absence of correlation between dipoles and orientation of permanent dipoles with the electric field results in significant dipole moment values. With an increase of the protein concentration, an antiparallel association of dipoles results in a decrease in the number of dipoles, which are oriented with the field. Thus the magnitude of the dipole moment is smaller under such conditions. Negative correlations between dipoles have been observed previously for proteins such as bovine serum albumin, and rod shaped collagen (44,45).

Antibody Flexibility

The major contribution to the dipole moment comes from the rotational relaxation time of the molecule. Antibody motions can be monitored by analyzing the relaxation time using dielectric dispersion curves. The dielectric relaxation times range from 30 ns to 200 ns for all the MAbs depending on the pH. The relaxation time of the protein depends upon the shape and volume given by the Stokes-Einstein equation (27):

$$\tau = \frac{4\pi ab^2}{kT}\eta\psi \tag{5}$$

where a and b are the minor and major axis of a spheroid, respectively, k is the Boltzmann constant (J/K), T is the temperature (K), η is the viscosity and ψ is the Perrin function (46), which is 1 for spherical proteins, when a=b (27). Antibodies consist of three independently folded compact globular domains connected through a flexible hinge region where the two heavy chains are held together by disulfide bridges. This arrangement allows the two Fab arms to assume different angles, θ, between 0 and 180°. Since the flexibility of the hinge region can result in multiple conformational states of an antibody, it can be expected that the Perrin function deviates from 1 for such molecules and depends heavily on

the angle between the two Fab fragments. Carrasco *et al.* (47) used frictional ratio data obtained from the determined sedimentation coefficients to calculate the Perrin function for IgG subclasses. The Perrin function obtained in this study suggested that the average value for θ to follow the trend $\theta_{IgG3} > \theta_{IgG1} > \theta_{IgG2} \sim \theta_{IgG4}$. Varying the pH may change the Perrin function and can be interpreted as change in the angle θ between Fab arms and hence a change in γ, the angle between the dipoles. For example, for the model of Mab1 having a more compact Y shaped conformation (higher Perrin function value), the calculated dipole moment is higher compared to the model of Mab1 having a more open Y shaped conformation (data not shown).

If all the domain motions of an antibody are faster than field oscillation, then the experimental measurement will be the time average that will equal the ensemble average. If some of the motions are slow relative to the field oscillations, then the experimental measurement will be the ensemble average that may or may not equal the time average, with the disparity varying with frequency. Therefore, it is difficult to decide if dipole moment can solely be explained by rotational relaxation of an antibody or if additional effects like intra-domain motions have to be included. Overall, the orientations of domain may vary depending upon the ionization of the charges (dependent on pKa and pH) and intra-domain interactions resulting in the specific dipole moment *versus* pH profiles.

Protein-Protein Interaction

A multitude of forces such as charge-charge interactions, charge-dipole interactions, dipole-dipole interactions, hydrophobic interactions and specific ion interactions govern protein properties in solution. Out of these, traditionally charge-charge interactions assume a net charge on the protein macroion at a given pH and thus these interactions as well as the excluded volume interactions are repulsive, while others are attractive in nature. Localized charge distributions, which may result in a net dipole moment or potential interactions of positive and negative charge patches, can result in attractive interactions. Overall, the relative magnitudes of the repulsive and attractive interactions can vary depending upon the distance between the molecules. Previously, dynamic and static light scattering, and ultrasonic rheology measurements (G′) have been used to probe the net interactions for the MAbs and charge-swap mutants (23).

Both G′and k_D values obtained from ultrasonic rheology and dynamic light scattering (DLS) studies, respectively, were found to vary with pH. The trend observed in G' and k_D *versus* pH (23) correlates well with the dipole moment *versus* pH trend. However, the question we had in mind was, which of the forces contribute most towards the pH maxima and minima as observed in the G′ and k_D studies, respectively? In dilute conditions, MAb1 showed net attractive interactions at pH 6.0 suggested by a negative k_D value of −19.79 (23). The storage modulus data indicate that the attractive interactions present in dilute conditions (<14 mg/ml) are applicable in concentrated solutions (125 mg/ml) as well (23). The contribution of the dipole moment to attractive interactions is evidenced by higher dipole moment at pH 6.5 for MAb1 and at pHs 7–8 for MAb2, which is consistent with increased values of G' at these pHs (Fig. 3, this manuscript and Fig. 2(b) in ref. 23). This can also be inferred from dielectric increment dependence on concentration as shown in (Fig. 5a). However, MAb2, M7 and M10 showed repulsive interactions at pH 6 as shown by positive values of k_D (Fig. 3 in Yadav *et al.* (23)). The dominance of repulsive interactions under the high concentration conditions (125 mg/mL) is also noticeable in the G′ studies (Fig. 2 in Yadav *et al.* (23)) Therefore, for MAb2 and the charge swap mutants, M7 and M10, but not MAb1, the dominance of repulsive interactions around pH 6 seems to outweigh the effect of the dipole-dipole attractive interactions. This is consistent with our dipole data that showed a smaller dipole magnitude (Fig. 3) and lesser concentration dependence of the dielectric increment for M7 with respect to MAb1 (Fig. 5a). MAb2 and M10 show behavior similar to M7. At pH 7.0, in dilute conditions and low ionic strength (DLS measurements) the trend of attractive interactions is MAb1 > M7 ≥ MAb2 ~ M10 (Fig. 3b in Yadav *et al.* (23)) When the concentration is increased to 125 mg/ml, the trend of the attractive interactions determined by G' measurements changed to MAb2 > MAb1 > M10 > M7 (Fig. 2b in Yadav *et al.* (23)). The different trends observed in the two studies suggest that forces are affected differently at low and high concentrations. The trend for the dipole moment at pH 7 and low ionic strength is MAb1 > MAb2 > M10 > M7. Thus, the G′ study showed a larger magnitude of attractive interactions for MAb2 compared to MAb1, whereas the dipole data suggest a larger magnitude of dipole attractions for MAb1 compared to Mab2 at pH 7.0. This changed trend at pH 7.0 suggests that net interactions in concentrated solution may involve dominance of short-range forces other than dipole interactions such as hydrophobic interactions. At pH 8, the highest dipole moment for MAb2 correlates well with the magnitude of G′, suggesting the dominance of dipole-dipole interactions in MAb2 solution.

CONCLUSIONS

The highest magnitude of the dipole moment for MAb1 observed at pH 6.5 suggests that the major contribution towards attractive interactions comes from dipole interactions. Similarly, MAb2 shows the dominance of dipole-dipole interactions at pH 8. This is the first experimental proof of the existence of dipole-dipole interactions occurring in antibody

solutions to explain the overall attractive protein-protein interactions and high viscosity observed at high concentrations. Furthermore, protein molecules with a high dipole moment tend to have a propensity to self-interact and align/orient. For MAb1 and MAb2, this physical ordering or alignment however is not strong enough to result in the generation of a discrete new phase. In other words, protein-protein interaction potential (parameter) though positive may not be sufficiently strong to form a new solid phase. Current results agree with the notion of the formation of protein networks in the solution. The results also reveal that the pattern and location of charged residues in the complementarity region is important in promoting these dipole-dipole interactions. The experimental relaxation times of MAbs also suggest a complex dependence of the dipole moment on the orientation of the different domains relative to each other. Future work will involve dipole moment measurement of Fab and Fc fragments to assess the role of flexibility of the inter-domain hinge region.

ACKNOWLEDGMENTS AND DISCLOSURES

The authors thank Genentech Inc. for providing antibodies and financial support for this study, and Mariya Pindrus for repeating some of the experiments.

REFERENCES

1. Harris RJ, Shire SJ, Winter C. Commercial manufacturing scale formulation and analytical characterization of therapeutic recombinant antibodies. Drug Dev Res. 2004;61:137–54.
2. Shire SJ, Shahrokh Z, Liu J. Challenges in the development of high protein concentration formulations. J Pharm Sci. 2004;93:1390–402.
3. Kanai S, Liu J, Patapoff TW, Shire SJ. Reversible self-association of a concentrated monoclonal antibody solution mediated by Fab-Fab interaction that impacts solution viscosity. J Pharm Sci. 2008;97:4219–27.
4. Liu J, Nguyen MDH, Andya JD, Shire SJ. Reversible self-association increases the viscosity of a concentrated monoclonal antibody in aqueous solution. J Pharm Sci. 2005;94:1928–40.
5. Hardy J, Selkoe DJ. The amyloid hypothesis of Alzheimer's disease: progress and problems on the road to therapeutics. Science. 2002;297:353–6.
6. Harper JD, Lansbury Jr PT. Models of amyloid seeding in Alzheimer's disease and scrapie: mechanistic truths and physiological consequences of the time-dependent solubility of amyloid proteins. Annu Rev Biochem. 1997;66:385–407.
7. Koo EH, Lansbury PT, Kelly JW. Amyloid diseases: abnormal protein aggregation in neurodegeneration. Proc Natl Acad Sci U S A. 1999;96:9989–90.
8. Uversky VN, Fink AL, editors. Protein misfolding, aggregation and conformational diseases, part B: molecular mechanisms of conformational diseases. Prot Rev. 2007;6.
9. Connolly BD, Petry C, Yadav S, Demeule B, Ciaccio N, Moore JMR, *et al.* Weak interactions govern the viscosity of concentrated antibody solutions: high-throughput analysis using the diffusion interaction parameter. Biophys J. 2012;103:69–78.
10. Saluja A, Kalonia DS. Nature and consequences of protein-protein interactions in high protein concentration solutions. Int J Pharm. 2008;358:1–15.
11. Yadav S, Shire SJ, Kalonia DS. Viscosity behavior of high-concentration monoclonal antibody solutions: correlation with interaction parameter and electroviscous effects. J Pharm Sci. 2012;101:998–1011.
12. George A, Chiang Y, Guo B, Arabshahi A, Cai Z, Wilson WW. Second virial coefficient as predictor in protein crystal growth. Methods Enzymol. 1997;276:100–10.
13. George A, Wilson WW. Predicting protein crystallization from a dilute-solution property. Acta Crystallogr D Biol Crystallogr. 1994;50:361–5.
14. Narayanan J, Liu XY. Protein interactions in undersaturated and supersaturated solutions: a study using light and x-ray scattering. Biophys J. 2003;84:523–32.
15. Wilson WW. Light scattering as a diagnostic for protein crystal growth—a practical approach. J Struct Biol. 2003;142:56–65.
16. Zhang J, Liu XY. Effect of protein-protein interactions on protein aggregation kinetics. J Chem Phys. 2003;119:10972–6.
17. Chari R, Jerath K, Badkar AV, Kalonia DS. Long- and short-range electrostatic interactions affect the rheology of highly concentrated antibody solutions. Pharm Res. 2009;26:2607–18.
18. Kumar V, Dixit N, Zhou LQ, Fraunhofer W. Impact of short range hydrophobic interactions and long range electrostatic forces on the aggregation kinetics of a monoclonal antibody and a dual-variable domain immunoglobulin at low and high concentrations. Int J Pharm. 2011;421:82–93.
19. Saluja A, Badkar AV, Zeng DL, Nema S, Kalonia DS. Ultrasonic storage modulus as a novel parameter for analyzing protein-protein interactions in high protein concentration solutions: correlation with static and dynamic light scattering measurements. Biophys J. 2007;92:234–44.
20. Yadav S, Shire SJ, Kalonia DS. Viscosity analysis of high concentration bovine serum albumin aqueous solutions. Pharm Res. 2011;28:1973–83.
21. Yadav S, Liu J, Shire SJ, Kalonia DS. Specific interactions in high concentration antibody solutions resulting in high viscosity. J Pharm Sci. 2010;99:1152–68.
22. Yadav S, Laue TM, Kalonia DS, Singh SN, Shire SJ. The influence of charge distribution on self-association and viscosity behavior of monoclonal antibody solutions. Mol Pharm. 2012;9:791–802.
23. Yadav S, Sreedhara A, Kanai S, Liu J, Lien S, Lowman H, *et al.* Establishing a link between amino acid sequences and self-associating and viscoelastic behavior of two closely related monoclonal antibodies. Pharm Res. 2011;28:1750–64.
24. Oncley JL. Electric moments and relaxation times of protein molecules. J Phys Chem. 1940;44:1103–13.
25. Oncley JL. The investigation of proteins by dielectric measurements. Chem Rev. 1942;30:433–50.
26. Oncley JL. The size, shape, and charge distribution of protein molecules. Science. 1947;106:509.
27. Desnica D. Self-association of hemoglobin: a dielectric dispersion study. Biopolymers. 1979;18:1685–90.
28. Gerber BR, Routledge LM, Takashima S. Self-assembly of bacterial flagellar protein: dielectric behavior of monomers and polymers. J Mol Biol. 1972;71:317–37.
29. Chari R, Singh SN, Yadav S, Brems DN, Kalonia DS. Determination of the dipole moments of RNAse SA wild type and a basic mutant. Proteins. 2012;80:1041–52.
30. Takashima S. Measurement and computation of the dipole moment of globular proteins III: chymotrypsin. Biophys Chem. 1996;58:13–20.
31. Cole KS, Cole RH. Dispersion and absorption in dielectrics. 1. Alternating-current characteristics. J Chem Phys. 1941;9:341–51.

32. Bonincontro A, De Francesco A, Onori G. Influence of pH on lysozyme conformation revealed by dielectric spectroscopy. Colloids Surf B. 1998;12:1–5.
33. Mellor BL, Cortes EC, Busath DD, Mazzeo BA. Method for estimating the internal permittivity of proteins using dielectric spectroscopy. J Phys Chem B. 2011;115:2205–13.
34. Hayashi Y, Miura N, Isobe J, Shinyashiki N, Yagihara S. Molecular dynamics of hinge-bending motion of IgG vanishing with hydrolysis by papain. Biophys J. 2000;79:1023–9.
35. Baker NA, Sept D, Joseph S, Holst MJ, McCammon JA. Electrostatics of nanosystems: application to microtubules and the ribosome. Proc Natl Acad Sci U S A. 2001;98:10037–41.
36. Dolinsky TJ, Nielsen JE, McCammon JA, Baker NA. PDB2PQR: an automated pipeline for the setup, execution, and analysis of Poisson-Boltzmann electrostatics calculations. Nuc Acids Res. 2004;32: W665–7.
37. Humphrey W, Dalke A, Schulten K. VMD: visual molecular dynamics. J Mol Graph Model. 1996;14:33–8.
38. Kirkwood JG, Shumaker JB. The influence of dipole moment fluctuations on the dielectric increment of proteins in solution. Proc Natl Acad Sci U S A. 1952;38:855–62.
39. Takashima S. Proton fluctuations in protein. Experimental study of the Kirkwood-Shumaker theory. J Phys Chem. 1965;69:2281–6.
40. Fricke H. The Maxwell-Wagner dispersion in a suspension of ellipsoids. J Phys Chem. 1953;57:934–7.
41. Schwarz G. The low-frequency dielectric dispersion of colloidal particles in electrolyte solution. J Phys Chem. 1962;66:2636–42.
42. Debye P. Molecular rotation in liquids. Phys Z. 1935;36:100–1.
43. Oleinikova A, Sasisanker P, Weingaertner H. What can really be learned from dielectric spectroscopy of protein solutions? A case study of ribonuclease A. J Phys Chem B. 2004;108:8467–74.
44. Moser P, Squire PG, O'Konski CT. Electric polarization in proteins–dielectric dispersion and Kerr effect. Isoionic bovine serum albumin. J Phys Chem. 1966;70:744–56.
45. Umemura S, Sakamoto M, Hayakawa R, Wada Y. Dielectric-relaxation of collagen in aqueous-solutions. Biopolymers. 1979;18:25–34.
46. Perrin F. Brownian movement of an ellipsoid. I. Dielectric dispersion of an ellipsoidal molecule. J Phys Radium. 1934;5:497–511.
47. Carrasco B, de la Torre Garcia J, Davis KG, Jones S, Athwal D, Walters C, *et al.* Crystallohydrodynamics for solving the hydration problem for multi-domain proteins: open physiological conformations for human IgG. Biophys Chem. 2001;93:181–96.